THE JOURNAL OF PHYSICAL CHEMISTRY C
Article
pubs.acs.org/JPCC

Theoretical Prediction of Phosphorene and Nanoribbons As Fast-Charging Li Ion Battery Anode Materials

Qiushi Yao,[†] Chengxi Huang,[†] Yongbo Yuan,[†] Yuzhen Liu,[†] Sumei Liu,[†] Kaiming Deng,*[,†] and Erjun Kan*[,†]

[†]Department of Applied Physics, and Key Laboratory of Soft Chemistry and Functional Materials (Ministry of Education), Nanjing University of Science and Technology, Nanjing, 210094, China

ABSTRACT: Ideal Li-ion battery materials should have a low diffusion barrier, which can realize fast charging/discharging. Here, density function theory (DFT) computations were performed to investigate the possibility of phosphorene and its nanoribbons as anode materials for Li-ion battery. Both phosphorene and its nanoribbons are direct band gap semiconductors, and show semiconductor-to-metal transition upon lithiation with significant charge transfer. Importantly, the computed energy barrier of Li diffuses on phosphorene monolayer along zigzag direction is only 0.09 eV, which indicates the possibility of ultrafast charging/discharging. Furthermore, the fast Li ion mobility is robust and well kept in phosphorene nanoribbons. The ultrahigh Li-ion mobility well distinguishes phosphorene from other typical two-dimensional (2D) materials, such as graphene and MoS_2, and makes phosphorene a promising anode material for Li ion batteries.

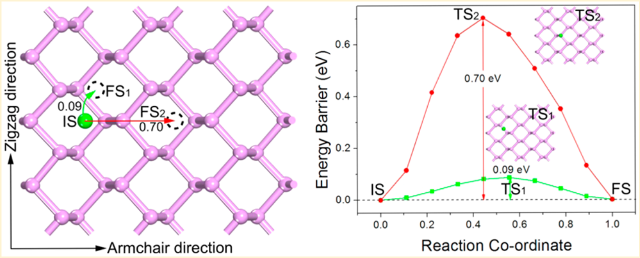

INTRODUCTION

Black phosphorus (BP) is the most stable phosphorus allotrope at room temperature that was first synthesized from white phosphorus under high pressure and high temperature in 1914.[1] It is a layered material coupled together by weak van der Waals (vdW) forces, structurally well resembles graphite. However, instead of a layered planar structure in graphite, BP is a puckered structure due to the sp^3 hybridization character of tetraphosphorus. Recently, two groups reported that bulk BP can be mechanically exfoliated to atomic layers which they called phosphorene.[2,3] Phosphorene turns out to be a promising material with wide potential applications. For example, phosphorene based field effect transistors (FETs) show a high charge-carrier mobility up to 1000 $cm^2V^{-1}s^{-1}$, much better than other typical two-dimensional (2D) semiconductors, such as MoS_2 (around 200 cm^2 V^{-1} s^{-1}).[3] In contract to graphene, phosphorene is a direct band gap semiconductor whose band gap strongly depending on the number of layers.[2,4] The band gap of BP can be monotonously tunable from ~0.3 eV in bulk to ~1.6 eV for a monolayer.[2,4] Additionally, the band gap can also be effectively modified by strain,[5−7] stack orders,[8] electric field[8] and so on. However, the most particularly characters of phosphorene are its high anisotropic electric conductance and optical responses,[2,4,5,9,10] which distinguish it from graphene and MoS_2.

On the other hand, 2D materials attract a lot of attention in the field of lithium-ion batteries (LIBs) because of their large surface-to-volume ratio and unique electronic properties. For today's LIBs, it is highly desired with high capacity and fast charging/discharging, which naturally requires strong binding and low diffusion barriers. Graphene and MoS_2 have been considered to be novel electrode materials for advanced LIBs.[11−15] Fan et al. have reported that Li atoms can be adsorbed on the hollow position with a large binding energy of 1.3 eV.[16] The large binding energy of Li atoms ensures its high capacity. However, they also demonstrated that the energy barrier of Li diffusion is around 0.3 eV, which significantly slow down the charging/discharging process. The same situation is also explored by Li et al. for MoS_2 layer.[14]

By carefully looking at the structures of graphene and MoS_2, we are not surprised that the diffusion barrier is slightly high. When moving on the surface, Li ions should cross the area with high electron density. Consequently, a moderate energy barrier is required. To accelerate the ions diffusion, it is necessary to find a suitable material with strong binding. Very recently, BP-carbon composite is demonstrated to be an attractive anode material with a long cycle life and high-rate capability.[17] BP-carbon bonds are stable during lithium insertion/extraction, maintaining excellent electrical connection between phosphorus and carbon.[17]

In consideration of the potential applications of phosphorene as anode materials for LIBs, it will be necessary and interesting to investigate the adsorption and diffusion of Li atoms on phosphorene. Here, we systematically explored the interaction between Li atoms and phosphorene by means of density functional theory (DFT) computations, and phosphorene monolayer, zigzag, and armchair nanoribbons were taken into account as the possible anode materials. It was found that Li atoms can bind to phosphorene via a moderate binging energy

Received: March 4, 2015
Published: March 9, 2015

DOI: 10.1021/acs.jpcc.5b02130
J. Phys. Chem. C 2015, 119, 6923−6928

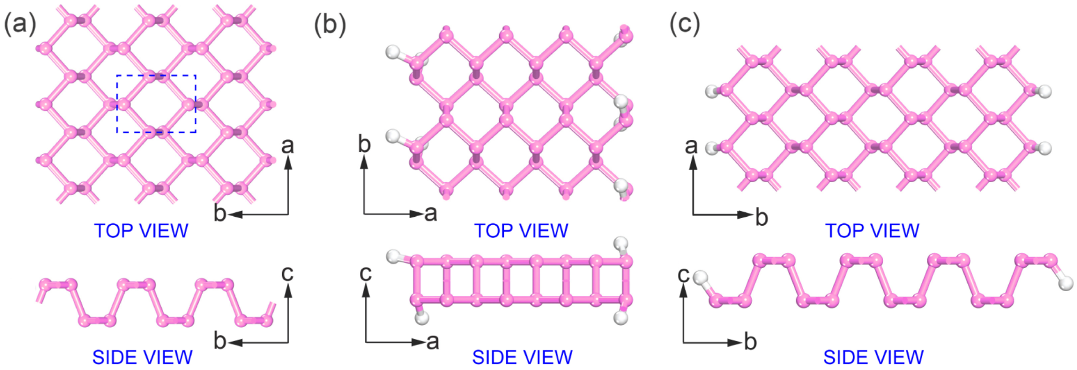

Figure 1. (a) Top and side view of phosphorene monolayer. Dashed rectangle denotes the primitive cell. (b) Top and side view of edge H-saturated 8-APNR. (c) Top and side view of edge H-saturated 8-ZPNR. The purple and white balls denote phosphorus and hydrogen atoms, respectively.

with significant electrons doping to phosphorene, leading to an insulator−metal transition. Additionally, the computed migration barriers of Li atoms diffuse along zigzag direction are about 0.09 eV, much lower than that on graphitic carbon (~0.3 eV)[18−20] and MoS_2 monolayer (~0.21 eV).[14] We also found that Li atoms prefer to diffuse along zigzag direction rather than diffuse along armchair direction, which can prevent the crystallization (such as dendrite formation) of Li atoms, making phosphorene based LIBs safer and longer circle-life than graphene and MoS_2 based LIBs. Because of the large diffusion energy barrier differences, the diffusion of Li on phosphorene is highly energetically favorable along the zigzag direction, while diffusion along the armchair direction is almost prohibited. In this case, Li atoms from one zigzag channel cannot cohere with Li atoms from another zigzag channel, thus preventing the crystallization of Li atoms.

■ COMPUTATIONAL METHODS

Our first-principles calculations were based on DFT with generalized gradient approximation (GGA)[21] for exchange correlation potential. Perdew−Burke−Ernzerholf (PBE) functional was used for the GGA as implemented in Vienna ab initio simulation package (VASP).[22] A 3 × 3 × 1 supercell was used to simulate Li adsorption on phosphorene monolayer. Distance between two adjacent Li atoms was around 10 Å, so interactions between two Li atoms can be ignored. At the same time, a vacuum space about 15 Å between phosphorene layers was used to avoid any interactions. The structures were relaxed without any symmetry constraints with a cutoff energy of 500 eV. The convergence criteria of energy and force were set to 1×10^{-5} eV and 0.01 eV/Å, respectively. Reciprocal space was represented by a Monkhorst−Pack special *k*-point scheme[23] with 3 × 3 × 1, 1 × 17 × 1, and 17 × 1 × 1 grid meshes for structure relaxation for phosphorene monolayer, armchair phosphorene nanoribbon (APNR) and zigzag phosphorene nanoribbon (ZPNR), respectively. Self-consistent field (SCF) computations were performed with *k*-points of 5 × 5 × 1, 1 × 19 × 1, and 19 × 1 × 1 for phosphorene monolayer, APNR and ZPNR, respectively. The accuracy of our procedure was tested by calculating the lattice constants and energy gap of phosphorene. Our calculated results of a = 3.30 Å, and b = 4.62 Å in line with previous study.[4] The energy gap of phosphorene monolayer was calculated to be 0.90 eV (Figure 2a) in good agreement with ref 7 (0.91 eV). The climbing image nudged elastic band (NEB)[24,25] was performed to find saddle points and minimum energy paths (MEPs) between a given initial state (IS) and final state (FS). The NEB method was known as an effectively tool for finding MEP and transition state (TS).[26,27]

■ RESULTS AND DISCUSSION

Electronic Structure of Pristine Phosphorene and Nanoribbons. Figure 1 illustrates geometric structures of phosphorene monolayer and PNRs. For PNRs, we selected 8-APNR and 8-ZPNR as the representative models. In our case, all of the nanoribbons were saturated by hydrogen atoms. Different from that of graphene or silicene, phosphorus atoms form covalent bonding with three adjacent atoms, and lead to a puckered honeycomb structure in phosphorene. The fluctuation character of phosphorene caused by sp^3 hybridization produces a higher and lower atomic layer.

As shown in Figure 2, phosphorene is a semiconductor with direct energy gap. The calculated band gap for phosphorene is about 0.9 eV, which agrees well with previous results. From the plotted partial charge density, we found that both the valence band maximum (VBM) and conduction band minimum (CBM) are contributed by the p_z orbital of phosphorus atoms. Furthermore, by cutting the monolayer structure into nanoribbons, we explored that the semiconducting character is well kept in PNRs. As shown in Figure 2, parts b and c, APNR and ZPNR have an energy gap of 1.18 and 1.55 eV, respectively. Similar with that of phosphorene, both the CBM and VBM are contributed by the p_z orbital of phosphorus atoms. But we also noticed that the existence of edge structures has greatly modified the partial charge distribution of CBM and VBM. For 8-ZPNR, both the VBM and CBM are contributed by the P atoms in the central region of the PNRs (Figure 2c). However, for 8-APNR, VBM is contributed by the central P atoms (Figure 2b), while CBM of 8-APNR contains little contribution from the edge P atoms (Figure 2b).

Now, we studied the possibility of single Li atom adsorption on phosphorene monolayer and PNRs. To avoid the interaction of Li atoms, we adopted a 3 × 3 × 1 supercell of phosphorene. From the geometric structure, there are two representative sites for Li atoms on phosphorene, namely, the hollow site (H) above the center of the triangle and the top site (T) directly above one P atom, which are denoted as H and T in Figure 3, parts a and b. At the H site, Li atom is coordinated by three P atoms, while at the T site Li atom is coordinated by only one P atom. By placing Li atoms at a different site, and relaxing the structure, we can calculate the binding energy from the equation $E_b = E_P + E_{Li} - E_{P+Li}$, where E_b is the binding energy of Li on monolayer phosphorene, E_P is the energy of phosphorene monolayer supercell without Li atom, E_{Li} is the

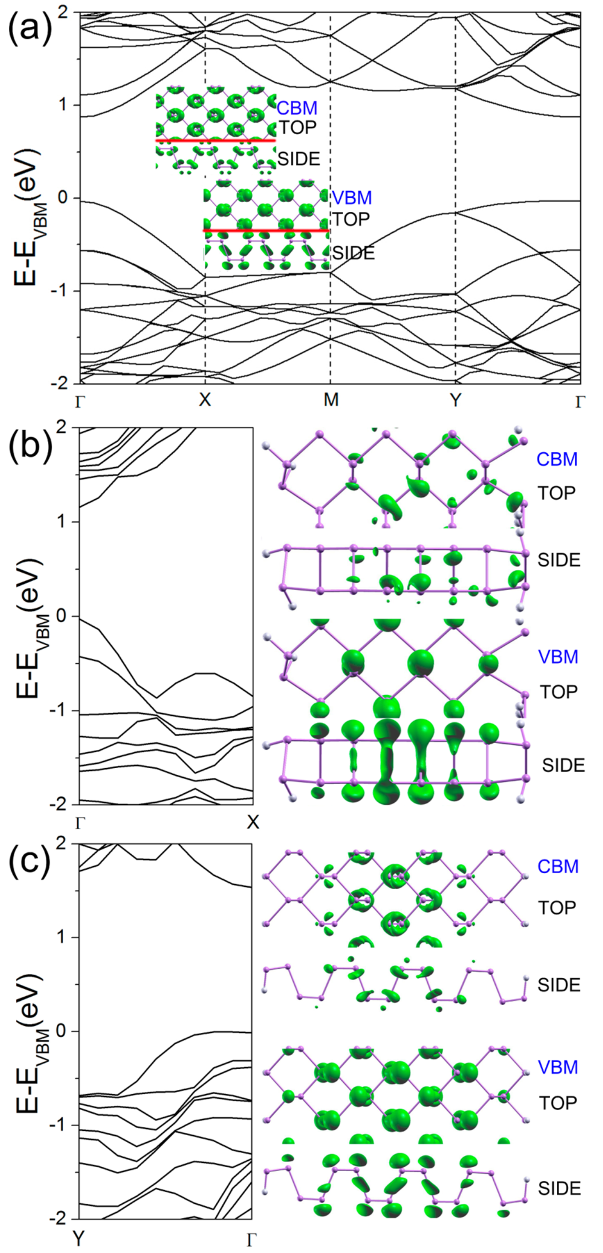

Figure 2. Calculated band structures and partial charge density of (a) monolayer phosphorene, (b) edge H-saturated 8-APNR, and (c) edge H-saturated 8-ZPNR. Γ = (0, 0, 0), X = (0, 0.5, 0), M = (0.5, 0.5, 0) and Y = (0.5, 0, 0). The purple and white balls denote phosphorus and hydrogen atoms, respectively.

energy of isolated Li atom, and E_{P+Li} is the total energy of Li-adsorbed phosphorene system.

Interestingly, we find that the Li atom cannot be adsorbed at the T site and will automatically move to the H site. The newly formed three Li−P bonds are 2.57, 2.57, and 2.48 Å. Since the three coordinated P atoms did not form an equilateral triangle, three Li−P bonds are not equal to each other. Similarly, we also defined the possible adsorptive sites for APNR and ZPNR as shown in Figure 3, parts c and d. As summarized in Table 1, the calculated binding energy of Li atom on phosphorene monolayer is 2.16 eV, much larger than Li adsorbs on monolayer graphene (1.04 eV)[28] and slightly larger than that of MoS_2 (2.12 eV).[14] As we know, enhanced Li adsorption indicates the increased capacity of battery. Logically, we can reasonably hypothesize that phosphorene has big potential to be the anode material of LIBs.

For 8-APNR, there are five possible adsorptive sites along zigzag direction, which are denoted as A_i (i = 1, 2, 3, 4, 5) in Figure 3c. While for 8-ZPNR, we can find seven possible adsorptive sites, defined as Z_i (i = 1, 2, 3, 4, 5, 6, 7) in Figure 3d. The calculated binding energies (see Table 1) indicate that Li ion is still strongly bound on PNRs, although the binding energy is slightly lower. Different with the case of MoS_2 nanoribbons, edge parts of PNRs are not preferred by the Li ion, as explored by the calculated binding energy. As demonstrated in Figure 2, we have shown that edge atoms do not have too much contribution to both CBM and VBM. Therefore, the adsorption of Li ion is weakened by the edge atoms.

Although pristine phosphorene and PNRs are semiconductor with an direct energy gap, the adsorption of Li atoms will significantly modify the electronic structure. As shown in Figure 4, phosphorene monolayer and PNRs undergo semiconductor-to-metal transitions upon lithiation. By means of differential charge density analysis (Figure 4, parts d, e and f), we can see significant electrons transfer from Li atom to phosphorene or PNRs, leading to the semiconductor-to-metal transition. In fact, according to Bader charge analysis,[29−31] Li possesses 0.88, 0.86, and 0.82 $|e|$ positive charge for phosphorene monolayer, 8-APNR and 8-ZPNR, respectively, indicating that there are certain ionic components in the newly formed Li−P bonds. Our researches indicate that Li atoms can bind to phosphorene monolayer and PNRs with moderate binding energies of about 2.0 eV.

Diffusion of a Single Li Atom on PNRs. In this part, we discussed the diffusion of a single Li atom on phosphorene monolayer and nanoribbons. First, we explored the diffusion of Li on phosphorene monolayer between two neighboring H sites, one along the zigzag direction and the other one along the armchair direction, as indicated in Figure 5(a). Surprisingly, the computed energy barrier along zigzag direction is only 0.09 eV, much lower than that along armchair direction (0.70 eV). It has been well explored that diffusion barrier determine the charging/discharging process for LIBs. From the calculated energy barrier along zigzag direction (0.09 eV), which is the lowest diffusion barrier in all low-dimensional materials, we suggest that phosphorene may be the anode materials of LIBs with the big potential for fast charging/discharging.

The calculated transition state (TS) along zigzag direction is Li adsorbed on the bridge site, while the TS along armchair direction is Li adsorbed on the T site (Figure 5b). According to Arrhenius equation, $D \propto \exp(E/kT)$, in which E is the energy barrier, k is the Boltzmann constant, and T is the temperature, we can quantitatively estimate that Li mobility along zigzag direction can be increased by a factor of 10^{10} compared with that along armchair direction at 300 K. It means that the diffusion of Li on phosphorene monolayer exhibits huge anisotropic feature. Combining with its electric conductance and optical responses,[2,4,5,9,10] high anisotropy may be the unique character of phosphorene in compare with other 2D materials, such as graphene and MoS_2.

The representative puckered structure may be the origin of its high anisotropy. Take a side view of phosphorene (Figure 1b); it looks like a mountain chain with regular valleys and peaks. Li atom prefers to move along valley rather than climb over the peak. This naturally raises an interesting question: if we cut phosphorene along the armchair direction or the zigzag

DOI: 10.1021/acs.jpcc.5b02130
J. Phys. Chem. C 2015, 119, 6923−6928

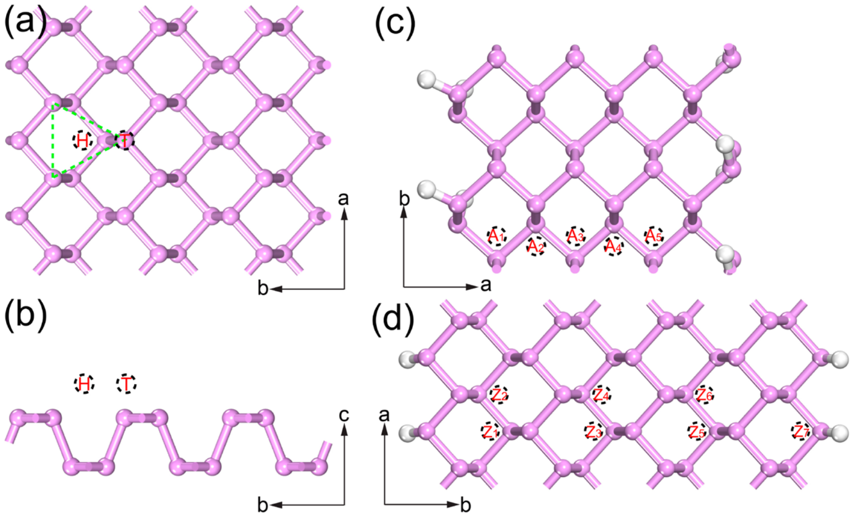

Figure 3. (a) Top and (b) side view of phosphorene monolayer. The dash line circles signed as H (hollow) and T (top) indicate two representative sites for Li atom to adsorb. (c) A_1 to A_5 denote the representative sites for Li atom to adsorbed on 8-APNR. (d) Z_1 to Z_7 denote the representative sites for Li atom to adsorbed on 8-ZPNR. The purple and white balls denote phosphorus and hydrogen atoms, respectively.

Table 1. Computed Li Binding Energies (E_b) in Electronvolts for All the Examined Li Adsorption Sites on Phosphorene Monolayer, 8-APNR and 8-ZPNR

site	H	A_1	A_2	A_3	A_4	A_5	Z_1	Z_2	Z_3	Z_4	Z_5	Z_6	Z_7
E_b	2.16	1.97	2.01	2.03	2.03	1.97	1.92	1.96	1.97	1.97	1.97	1.97	1.41

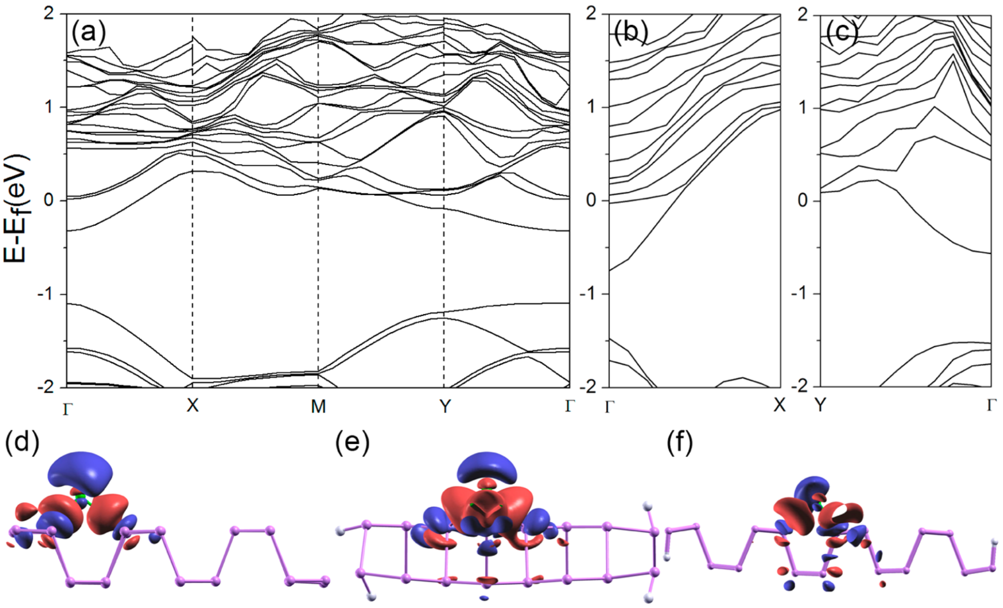

Figure 4. Calculated band structures of (a) phosphorene monolayer with Li adsorbed on H site, (b) 8-APNR with Li adsorbed on A_3 site, and (c) 8-ZPNR with Li adsorbed on Z_4 site. Differential charge density with an isosurface value of 0.01 e/Å^3 for (d) phosphorene monolayer, (e) 8-APNR, and (f) 8-ZPNR. The red and blue regions indicate an increase and decrease in electron density, respectively. The purple, green, and white balls denote phosphorus, lithium, and hydrogen atoms, respectively.

direction, could the high anisotropy and low diffusion barrier still exist?

To investigate the mobility of Li atoms along armchair 8-APNR, we constructed a supercell two times large of 8-APNR primitive cell. Another five representative sites marked as A-*i* (*i* = 1, 2, 3, 4, 5) are available along armchair direction. The energy barriers corresponding to different migration paths are indicated in Figure 5c. Importantly, we found that energy barrier along zigzag direction is still very low. It means that Li atoms prefer to move perpendicularly to the nanoribbon direction rather than move along the nanoribbon direction. According to the difference between the energy barriers, Li mobility along zigzag direction can also be 10^{10} times larger than that along armchair direction at 300 K, in line with Li diffusion on phosphorene monolayer.

Finally, we studied the diffusion of Li atoms on 8-ZPNR. The diffusion of Li atoms on 8-ZPNR also shows high anisotropic character according to the computed migration barriers. By

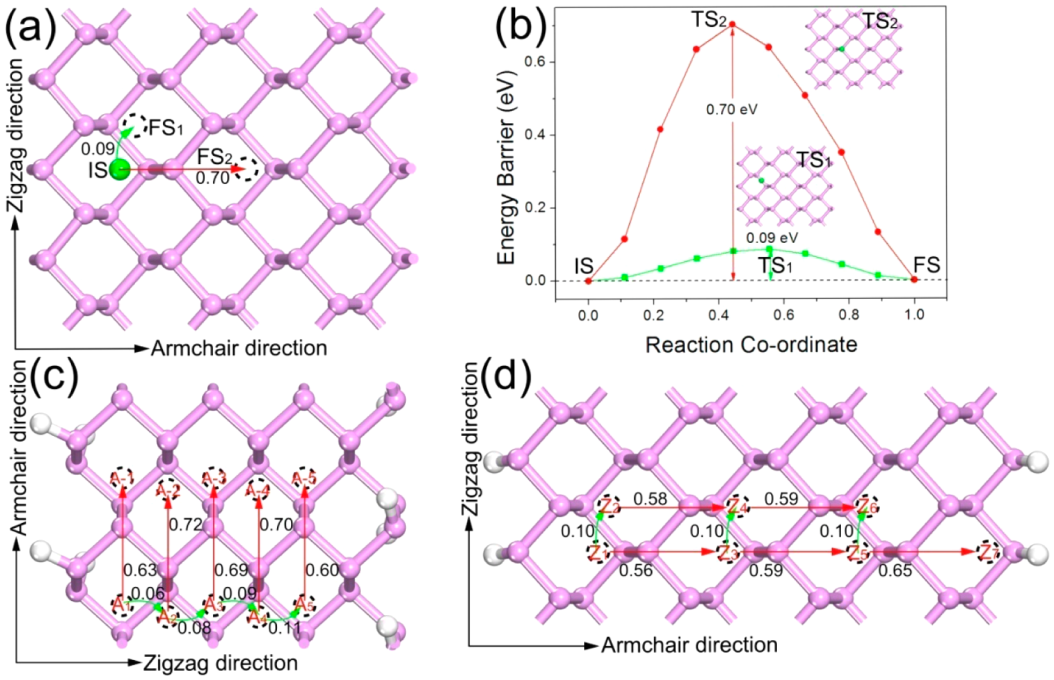

Figure 5. (a and b) Diffusion path and barriers of Li on phosphorene monolayer. (c) Diffusion path and barriers of Li on 8-APNR. (d) Diffusion path and barriers of Li on 8-ZPNR. Crooked green and straight red arrows denote Li atom migrates along zigzag and armchair directions, respectively. The purple, green, and white balls denote phosphorus, lithium, and hydrogen atoms, respectively. The numbers indicate the diffusion barriers in electronvolts.

means of Arrhenius equation, the estimated difference of Li mobility between two directions would be 10^9 at 300 K. And more importantly, we also found that the diffusion barrier along zigzag direction is still around 0.1 eV. So we come to the conclusion that both the low diffusion barrier and the high anisotropy of Li atoms diffusion are robust no matter if they are on phosphorene monolayer or PNRs.

CONCLUSIONS

To summarize, we performed DFT computations to disclose the Li adsorption and diffusion on phosphorene monolayer, APNR and ZPNR. Our results demonstrated that Li atoms can bind to phosphorene with a binding energy about 2.00 eV. Both phosphorene monolayer and PNRs undergo a transition from semiconductor to metal upon Li adsorbed with significant electrons doping to phosphorene. On the other hand, the diffusion of Li atoms on phosphorene shows high anisotropic character and low energy barriers no matter on phosphorene monolayer or PNRs. Combining with its electric conductance and optical responses, low diffusion barrier and high anisotropy may be a particular character of phosphorene upon lithiation. Importantly, the moderate binding energy (~2.00 eV) and tiny migration energy barrier (~0.10 eV along the zigzag direction) of Li atoms on phosphorene make it a potential candidate as anode materials for LIBs.

AUTHOR INFORMATION

Corresponding Authors

*(K.D.) E-mail: kmdeng@njust.edu.cn.
*(E.K.) E-mail: ekan@njust.edu.cn.

Notes

The authors declare no competing financial interest.

ACKNOWLEDGMENTS

This work was supported by the NSFC (21203096, 11374160, 21403111), by the National Basic Research Program of China (2014CB931700/2014CB931702), by the NSF of Jiangsu Province (BK20130031, BK2012392, BK2012394), by New Century Excellent Talents in University (NCET-12-0628), by the Qinglan Project of Jiangsu Province, and by the Innovation Program of Jiangsu Province (KYLX_0355). We also acknowledge the support from the Shanghai Supercomputer Center.

REFERENCES

(1) Bridgman, P. W. *J. Am. Chem. Soc.* **1914**, *36*, 1344.

(2) Liu, H.; Neal, A. T.; Zhu, Z.; Luo, Z.; Xu, X.; Tománek, D.; Ye, P. D. *ACS Nano* **2014**, *8*, 4033.

(3) Li, L.; Yu, Y.; Ye, G. J.; Ge, Q.; Ou, X.; Wu, H.; Feng, D.; Chen, X. H.; Zhang, Y. *Nat. nanotechnol.* **2014**, *9*, 372.

(4) Qiao, J.; Kong, X.; Hu, Z. X.; Yang, F.; Ji, W. *Nat. Commun.* **2014**, *5*, 4475.

(5) Fei, R.; Yang, L. *Nano Lett.* **2014**, *14*, 2884.

(6) Han, X.; Morgan Stewart, H.; Shevlin, S. A.; Catlow, C. R. A.; Guo, Z. X. *Nano Lett.* **2014**, *14*, 4607.

(7) Rodin, A. S.; Carvalho, A.; Castro Neto, A. H. *Phys. Rev. Lett.* **2014**, *112*, 176801.

(8) Dai, J.; Zeng, X. C. *J. Phys. Chem. Lett.* **2014**, *5*, 1289.

(9) Tran, V.; Soklaski, R.; Liang, Y.; Yang, L. *Phys. Rev. B* **2014**, *89*, 235319.

(10) Xia, F.; Wang, H.; Jia, Y. *Nat. Commun.* **2014**, *5*, 4458.

(11) Chang, K.; Chen, W. *Chem. Commun.* **2011**, *47*, 4252.

(12) Chang, K.; Chen, W. *J. Mater. Chem.* **2011**, *21*, 17175.

(13) Chang, K.; Chen, W.; Ma, L.; Li, H.; Li, H.; Huang, F.; Xu, Z.; Zhang, Q.; Lee, J. *J. Mater. Chem.* **2011**, *21*, 6251.

(14) Li, Y. F.; Wu, D. H.; Zhou, Z.; Cabrera, C. R.; Chen, Z. F. *J. Phys. Chem. Lett.* **2012**, *3*, 2221.

(15) Park, K. H.; Lee, D.; Kim, J.; Song, J.; Lee, Y. M.; Kim, H. T.; Park, J. K. *Nano Lett.* **2014**, *14*, 4306.

DOI: 10.1021/acs.jpcc.5b02130
J. Phys. Chem. C 2015, 119, 6923−6928

(16) Fan, X.; Zheng, W.; Kuo, J. *ACS Appl. Mater. Interfaces* **2012**, *4*, 2432.
(17) Sun, J.; Zheng, G.; Lee, H. W.; Liu, N.; Wang, H.; Yao, H.; Yang, W.; Cui, Y. *Nano Lett.* **2014**, *14*, 4573.
(18) Toyoura, K.; Koyama, Y.; Kuwabara, A.; Tanaka, I. *J. Phys. Chem. C* **2010**, *114*, 2375.
(19) Persson, K.; Sethuraman, V. A.; Hardwick, L. J.; Hinuma, Y.; Meng, Y. S.; van der Ven, A.; Srinivasan, V.; Kostecki, R.; Ceder, G. *J. Phys. Chem. Lett.* **2010**, *1*, 1176.
(20) Persson, K.; Hinuma, Y.; Meng, Y. S.; Van der Ven, A.; Ceder, G. *Phys. Rev. B* **2010**, *82*, 125416.
(21) Perdew, J. P.; Burke, K.; Ernzerhof, M. *Phys. Rev. Lett.* **1996**, *77*, 3865.
(22) Kresse, G.; Furthmüller, J. *Phys. Rev. B* **1996**, *54*, 11169.
(23) Monkhorst, H. J.; Pack, J. D. *Phys. Rev. B* **1976**, *13*, 5188.
(24) Henkelman, G.; Jonsson, H. *J. Chem. Phys.* **2000**, *113*, 9978.
(25) Henkelman, G.; Uberuaga, B. P.; Jónsson, H. *J. Chem. Phys.* **2000**, *113*, 9901.
(26) Mills, G.; Jónsson, H. *Phys. Rev. Lett.* **1994**, *72*, 1124.
(27) Mills, G.; Jónsson, H.; Schenter, G. K. *Surf. Sci.* **1995**, *324*, 305.
(28) Uthaisar, C.; Barone, V.; Peralta, J. E. *J. Appl. Phys.* **2009**, *106*, 113715.
(29) Henkelman, G.; Arnaldsson, A.; Jónsson, H. *Comput. Mater. Sci.* **2006**, *36*, 354.
(30) Tang, W.; Sanville, E.; Henkelman, G. *J. Phys.: Condens. Matter.* **2009**, *21*, 084204.
(31) Sanville, E.; Kenny, S. D.; Smith, R.; Henkelman, G. *J. Comput. Chem.* **2007**, *28*, 899.